

Giant nonlinear magnetic response in a molecule-based magnet

Masaki Mito,* Kazuyuki Iriguchi, Hiroyuki Deguchi, and Jun-ichiro Kishine
Faculty of Engineering, Kyushu Institute of Technology, Kitakyushu 804-8550, Japan

Koichi Kikuchi

Department of Chemistry, Tokyo Metropolitan University, Hachioji, Tokyo 192-0397, Japan

Hiroyuki Ohsumi

Riken, SPring-8 Center, Sayo, Hyogo 679-5148, Japan

Yusuke Yoshida and Katsuya Inoue†

Department of Chemistry and Institute for Advanced Materials Research, Hiroshima University, Higashihiroshima 739-8526, Japan

(Received 3 August 2008; revised manuscript received 28 November 2008; published 22 January 2009)

We observed a giant nonlinear magnetic response in a molecule-based magnet, $[\text{Cr}(\text{CN})_6][\text{Mn}(R)\text{-pnH}(\text{H}_2\text{O})](\text{H}_2\text{O})$, in which single chiral ligands $[(R)\text{-pn's}]$ construct intermolecular network. The giant nonlinear magnetic response occurs at slightly higher temperature side of the magnetic ordering temperature. The existence of giant nonlinear response yields quite strange shape of the superconducting quantum interference device response against ac magnetic field. This response does not appear in the racemic system involving two kinds of chiral ligands $[(R)\text{-pn}$ and $(S)\text{-pn}]$, suggesting that the crystallographic chirality plays a crucial role in the occurrence of the giant nonlinear response.

DOI: [10.1103/PhysRevB.79.012406](https://doi.org/10.1103/PhysRevB.79.012406)

PACS number(s): 75.50.Xx, 75.25.+z, 75.40.Gb

Systematic fabrication of metal complex magnets using appropriate building blocks and intermediate organic ligands has established an important field of molecule-based magnets, which has resulted in the creation of numerous ferromagnets and/or ferrimagnets with optical transparency and high transition temperatures.^{1,2} The selections of metallic ions and organic ligands realize varied material syntheses for the production of multifunctionality. Recently, material design using a chiral organic ligand enabled to intentionally construct crystallographic chiral symmetry,^{3,4} and this research field has attracted much attention from researchers in the field of magneto-optical science.⁵ In particular, magnetochiral dichroism (MChD) effect⁶ is quite promising in the industrial application when the target material has the large magnetic moments. In this instance, “chirality” means “single-handedness,” and is used to describe a single-handed helical structure, i.e., either right or left handed (R or S style in the field of chemical synthesis). In this Brief Report, we represent an aspect of magnetic property in a molecule-based magnet with single chiral ligand.

The present target compound $[\text{Cr}(\text{CN})_6][\text{Mn}(R)\text{-pnH}(\text{H}_2\text{O})](\text{H}_2\text{O})$ [$(R)\text{-pn}$; $(R)\text{-1,2-diaminopropane}$] is well known in the field of molecule-based magnets as a prototype compound with chiral structural symmetry.³ The crystal structure is shown in Fig. 1, where Cr^{3+} and Mn^{2+} are shown in brown and purple, respectively. The $(R)\text{-pn}$ is attached to the Mn^{2+} ion via the nitrogen atom (shown in blue). It becomes a bimetallic ferrimagnet with total spin of $5/2$ (Mn^{2+}) $- 3/2$ (Cr^{3+}) $= 1$.³ Crystallographically, this system belongs to the orthorhombic space group $P2_12_12_1$ and there exists twofold helical axis along each principal crystal axis. Independently of the chirality of organic ligand, the green needlelike single crystals are obtained and we term these crystals as the green needle (GN). Hereafter, the GN involving single $R\text{-pn}$ is abbreviated

as $R\text{-GN}$. There were no distinct differences in physical properties (crystal structure and magnetism) between the $R\text{-GN}$ and $S\text{-GN}$, except for the chirality of 1,2-diaminopropane. Data on the dc magnetization have suggested that $R(S)\text{-GN}$ exhibits magnetic ordering at $T=37$ K, which turns out to be untrue later, and becomes a soft magnet with a saturation field of about 30 Oe at low temperature.³ Neutron diffraction experiments using the powder sample⁷ and single crystal⁸ have revealed that the target material is a noncollinear ferrimagnet with an easy axis along the a axis. In the μSR experiment, it was found that a pair of crystallographic enantiomers also had magnetic enantiomorphic symmetry.⁹

In the present Brief Report, we report the observation of a giant nonlinear magnetic response in $R\text{-GN}$. This response did not appear in the racemic system (rac-GN), where $R\text{-pn}$ and $S\text{-pn}$ were mixed in the process of synthesis with equal percentage.¹⁰ The space group of rac-GN is $P2_1/m$, where the structural chirality is lost owing to the existence of mirror symmetry perpendicular to a twofold helical axis. As described later, the giant nonlinear response in $R\text{-GN}$ is not due to static magnetic order.

Under an ac field of $H_{\text{ac}}=h \cos \omega t$, magnetization M is expanded as

$$M(t) = M_{1\omega} \cos \omega t + M_{2\omega} \cos 2\omega t + M_{3\omega} \cos 3\omega t + \cdots, \quad (1)$$

where ω is the angular frequency and $M_{n\omega}=h\chi_{n\omega}$ (n : integer) stands for the n th-harmonic component. In an actual system, there is often the delay of the ac response against the ac field, resulting in the occurrence of an out-of-phase component. However, it is herein assumed that the ac response appears without any delay against the ac field for simplicity of the

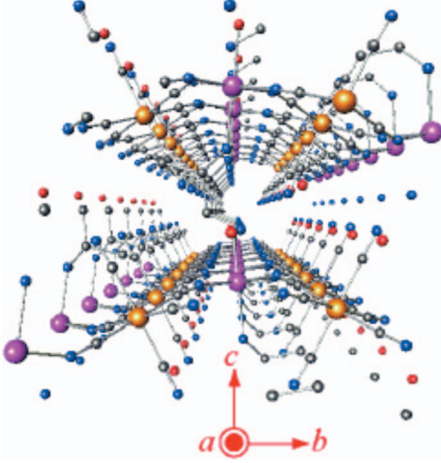


FIG. 1. (Color) Crystal structure of $[\text{Cr}(\text{CN})_6][\text{Mn}(R)\text{-pnH}(\text{H}_2\text{O})](\text{H}_2\text{O})$, wherein which Cr^{3+} is shown in brown, Mn^{2+} in purple, C in gray, and N in blue.

explanation. The series expansion of the magnetization M with general magnetic field H yields

$$M = \chi^{(0)}H + \chi^{(1)}H^2 + \chi^{(2)}H^3 + \chi^{(3)}H^4 + \dots, \quad (2)$$

where $\chi^{(0)}$ is the linear susceptibility and $\chi^{(m)}$ ($m \neq 0$) is the nonlinear susceptibility. The power expansion with cosine function after replacing H of Eq. (2) with $h \cos \omega t$ yields

$$\chi_{1\omega} = \chi^{(0)} + \frac{3}{4}\chi^{(2)}h^2 + \frac{5}{8}\chi^{(4)}h^4 + \dots,$$

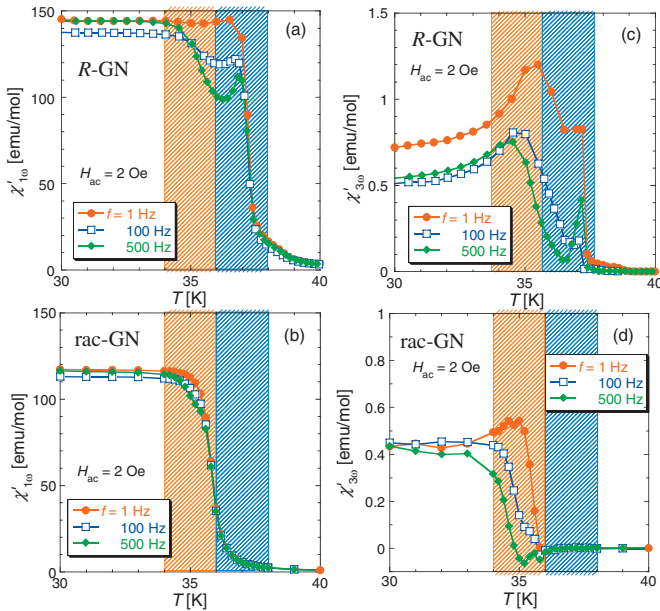


FIG. 2. (Color) In-phase components of the 1ω and 3ω magnetic susceptibilities, [(a),(b)] $\chi'_{1\omega}$ and [(c),(d)] $\chi'_{3\omega}$, respectively, for polycrystalline samples of the [(a),(c)] R and [(b),(d)] racemic forms of GN. The amplitude of the ac field is 2 Oe and the frequency is $f=1, 10, \text{ or } 100$ Hz.

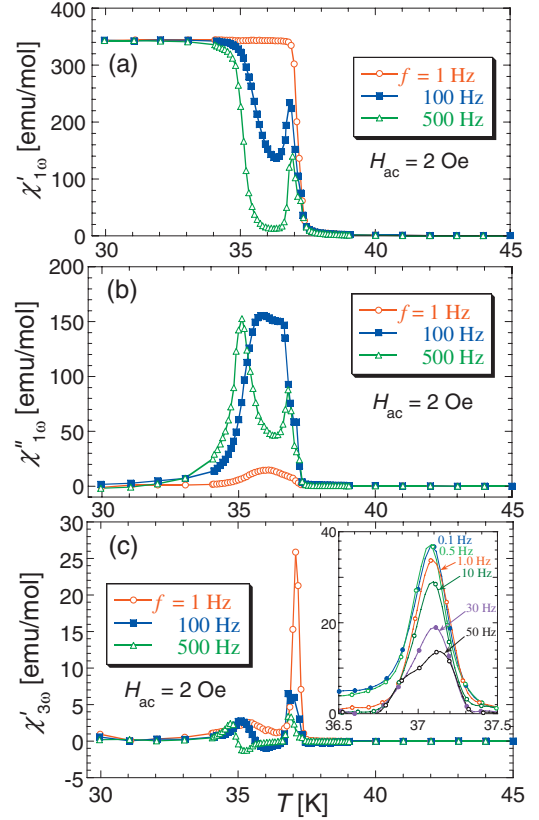


FIG. 3. (Color) Frequency dependencies of the [(a),(b)] in-phase and out-of-phase 1ω magnetic susceptibilities and the (c) in-phase 3ω magnetic susceptibility of R -GN in an ac field with an amplitude of 2 Oe applied along the a axis.

$$\chi_{2\omega} = \frac{1}{2}\chi^{(1)}h + \frac{1}{2}\chi^{(3)}h^3 + \dots,$$

$$\chi_{3\omega} = \frac{1}{4}\chi^{(2)}h^2 + \frac{5}{16}\chi^{(4)}h^4 + \dots. \quad (3)$$

In small h , the first harmonic $\chi_{1\omega}$ mainly reflects a linear response $\chi^{(0)}$, while the second $\chi_{2\omega}$ and the third $\chi_{3\omega}$ are intrinsically connected with $\chi^{(1)}$ and $\chi^{(2)}$, respectively. The $\chi^{(1)}$ ($\chi_{2\omega}$) is connected to the breaking of time inversion symmetry, and the large signal reflects the existence of spontaneous magnetization. The $\chi^{(2)}$ ($\chi_{3\omega}$) is connected to the breaking of spatial symmetry, and the anomaly verifies the occurrence of the long-ranged magnetic order (accompanying the large phase change) or the glassy state (not accompanying the large phase change).^{11–13} Thus, $\chi^{(2)}$ ($\chi_{3\omega}$) is an effective tool for clarifying the nature of the spin-environment interaction.¹⁴ Generally we can detect any information of magnetic aggregate over a finite spatial scale, i.e., magnetic domain, via the measurement of $\chi^{(2)}$ ($\chi_{3\omega}$).

The ac magnetic-susceptibility measurements were carried out using a superconducting quantum interference device (SQUID) magnetometer (Quantum Design, MPMS). The residual dc field (H_r) was carefully reduced down to less than 1% of the earth field, since the existence of large H_r makes the interpretation of $\chi_{n\omega}$ based on Eq. (3) quite com-

plex; odd $\chi^{(m)}$'s appear in odd $\chi_{n\omega}$ as well and even $\chi^{(m)}$'s do in even $\chi_{n\omega}$ too. A series of harmonic components $\chi_{n\omega}(=M_{n\omega}/h)$ was detected based on the Fourier transformation of the SQUID voltage.

Figure 2 shows the temperature dependencies of in-phase components of the 1ω and 3ω magnetic susceptibilities, $\chi'_{1\omega}$ [(a) and (b)] and $\chi'_{3\omega}$ [(c) and (d)], when polycrystalline samples of *R*-GN [(a) and (c)] and rac-GN [(b) and (d)] were used. The amplitude of the ac field was 2 Oe at frequency (f) of 1, 10, or 100 Hz. Considering the magnetic properties in the $\chi'_{1\omega}$ of *R*-GN, there were at least two anomalies at about 35 and 37 K. These splittings became more prominent with increasing frequency. The latter response showed remarkable frequency dependence, while the former response was insensitive to the change in frequency. With increasing frequency, the existence of the magnetic anomaly at 37 K becomes more prominent. The above-mentioned behaviors have been indeed confirmed by measurement of $\chi'_{1\omega}$ for *S*-GN.¹⁵ In contrast, the data for $\chi'_{3\omega}$ revealed the existence of multiple anomalies even at low frequencies. When the above-described magnetic behavior of *R*-GN was compared with that of rac-GN, we noticed that the anomaly that corresponded to that at 37 K for *R*-GN was not present for rac-GN. However, at around 35 K, the anomaly that was relatively stable in terms of frequency change was observed for both the *R*-GN and rac-GN. Thus, we can mention that the magnetic anomaly at 37 K is connected to the crystallographic chirality in *R*-GN.

Figure 3 shows the frequency dependencies of $\chi'_{1\omega}$, $\chi''_{1\omega}$, and $\chi'_{3\omega}$ of *R*-GN on the $H_{ac}(h=2 \text{ Oe})\parallel a$ axis. The a axis is a magnetic easy axis, and a large 3ω response appeared at the $H_{ac}\parallel a$ axis. For reference, it is noted that the $\chi_{2\omega}$ component was not detected with the accuracy more than a meaningful level. It means that the spontaneous magnetic moment is almost zero owing to a quite small residual field, and $\chi_{3\omega}$ ideally reflects $\chi^{(2)}$. In the 1ω responses ($\chi'_{1\omega}$ and $\chi''_{1\omega}$), an anomaly splits to at least two anomalies with increasing frequency, suggesting there are varied dynamic magnetic properties at around 35–37 K. However, the 3ω response exhibits at least two anomalies, even at ac fields of low frequency, as mentioned in the results of Fig. 2. The giant nonlinear magnetic response of $\chi'_{3\omega}$ at 37.0 K at $f=1$ Hz was systematically suppressed with increasing frequency and was not accompanied by any distinct anomaly of $\chi'_{1\omega}$. In contrast, the hump of $\chi'_{3\omega}$ at 35–36 K consisted of two anomalies. These anomalies split with increasing frequency. The upper anomaly at around 35.5 K was confirmed to have a resonating phenomenon at $f=3$ –6 Hz. The anomaly at 35 K persisted even at $f=500$ Hz, and the shape of the anomaly reflects the remarkable change of phase. In consequence, we can conclude that the anomaly at 35 K reflects the formation of long-range magnetic ordering. Thus, the above-mentioned difference of frequency dependence reveals that the spatial symmetry of magnetic moment at each magnetic anomaly at 35–37 K is intrinsically different. The results of Fig. 2 revealed that the 3ω responses at 35 and 35.5 K appeared in the racemic system, whereas there was no anomaly at 37 K.¹⁰ A series of nonlinear responses was not observed as a meaningful level of signal for the $H_{ac}\parallel b$ and c axes, where the intensity of $\chi'_{1\omega}$ was less than 2% of that for

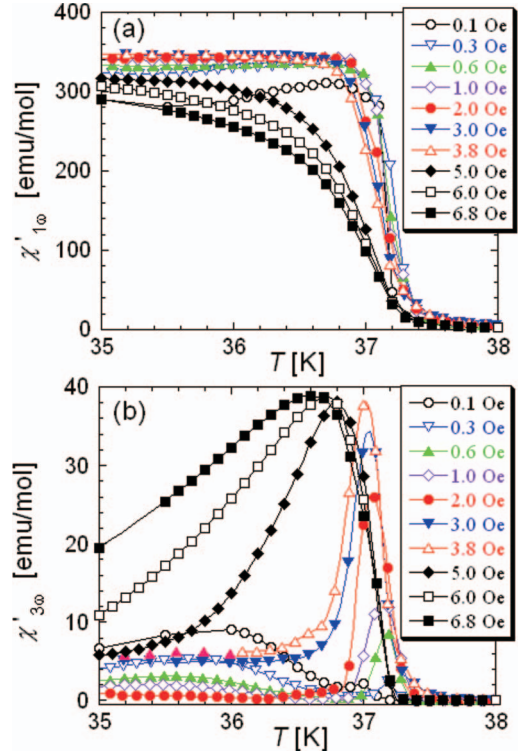


FIG. 4. (Color) ac field amplitude dependencies of the in-phase (a) 1ω and (b) 3ω magnetic susceptibilities of *R*-GN against an ac field applied along the a axis with a frequency of $f=1$ Hz.

$H_{ac}\parallel a$ axis. Now that of Fig. 3 represents that the nonlinear anomaly at 37 K in *R*-GN is giant at $H_{ac}\parallel a$ axis and it is due to neither static magnetic ordering nor familiar magnetic domain seen in spin-glass system, etc.

Figure 4 shows the ac field dependence of $\chi'_{1\omega}$ and $\chi'_{3\omega}$ of *R*-GN at $f=1$ Hz for the $H_{ac}\parallel a$ axis. In this instance, we ensured that the maximum field (6.8 Oe) was much lower

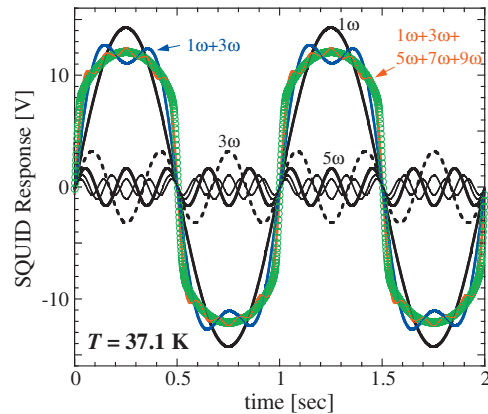


FIG. 5. (Color) SQUID response of *R*-GN against an external oscillating field of $h=6.8$ Oe and $f=1.0$ Hz at 37.1 K under the proper SQUID gain in the condition of $H_{ac}\parallel a$ axis. The green circles represent the observational data. The five black curves express the 1ω , 3ω , 5ω , 7ω , and 9ω responses, respectively. The response at 37.1 K cannot be analyzed with either 1ω alone or $1\omega+3\omega$. The U-shaped response is reproduced almost entirely using a linear combination up to at least 9ω .

than the saturation field (ca. 30 Oe). The field of $h=2$ Oe was sufficient to cause $\chi'_{3\omega}$ to exceed $\chi'_{1\omega}$ by about 10% at 37 K. For $h \geq 3.8$ Oe, the magnitude of the 1ω response was suppressed with increases in the ac field, while the 3ω response increased as the peak position shifted toward the lower-temperature side. As a consequence, the $\chi'_{3\omega}/\chi'_{1\omega}$ ratio increased with increasing ac field amplitude and then the actual magnetic response of the SQUID is extremely strange. For instance, at $H_{ac} \parallel a$ axis ($h=6.8$ Oe and $f=1$ Hz), the SQUID response at 37.1 K was U-shaped (Fig. 5), which is almost reproduced with a linear combination of odd components up to at least 9ω . Thus, the ratio of the amplitudes $1\omega:3\omega:5\omega:7\omega:9\omega$ was 14.27:3.20:1.67:1.05:0.70. This appearance of a series of odd harmonics justifies taking $\chi^{(2)}$ into consideration. Our series of analytic results indicates that the ratio of $\chi'_{3\omega}$ to $\chi'_{1\omega}$ continued to increase in the studied ac field region. For $h=6.8$ Oe, the magnitude of the 3ω response at 37 K approached 24% of 1ω . For a spin-glass system, $\chi_{3\omega}$ is generally 3 or 4 orders lower than $\chi_{1\omega}$ and is at most a few percent of $\chi_{1\omega}$.^{12,16} We wish to point out that the 3ω response of the studied compound was surprisingly large. As a condition for giant nonlinear response, the magnetic softness is important, whereas the microscopic mecha-

nism of the giant nonlinear response is not clear at present. However, at least, we can conclude that the crystallographic chirality plays a crucial role because the response was observed only in the crystallographically chiral crystal. Indeed, we have also observed the giant nonlinear magnetic response in a similar molecule-based magnet, $[\text{Mn}(R)\text{-pn}][\text{Cr}(\text{CN})_6][\text{Mn}(R)\text{-pn}_2(\text{H}_2\text{O})]_{0.5}(\text{H}_2\text{O})_{1.5}$, with single chiral ligand and hexagonal space group $P6_5$.

In summary, we described a giant second-order nonlinear magnetic response in a molecule-based chiral ferrimagnet $[\text{Cr}(\text{CN})_6][\text{Mn}(R)\text{-pnH}(\text{H}_2\text{O})](\text{H}_2\text{O})$, which was called R-GN. The magnitude of the nonlinear susceptibility response is extraordinary compared to those of previous experimental examples in the spin-glass system. We have not confirmed the distinct idea about the mechanism, but it is true that the nonlinear response detects any soft magnetic degrees of freedom formed over a wide spatial region prior to the magnetic ordering. The crystallographic chirality plays a crucial role in the occurrence.

This work was supported by a Grant-in-Aid for Scientific Research (A) (Contract No. 18205023) from the MEXT of Japan.

*mitoh@tobata.isc.kyutech.ac.jp

†kxi@hiroshima-u.ac.jp

¹O. Kahn, *Molecular Magnetism* (VCH, New York, 1993).

²K. Itoh and M. Kinoshita, *Molecular Magnetism* (Gordon and Breach, New York, 2000).

³K. Inoue, K. Kikuchi, M. Ohba, and H. Ōkawa, *Angew. Chem., Int. Ed.* **42**, 4810 (2003).

⁴H. Kumagai and K. Inoue, *Angew. Chem., Int. Ed.* **38**, 1601 (1999).

⁵G. L. J. A. Rikken and E. Raupach, *Nature (London)* **390**, 493 (1997).

⁶G. Wagniere, *Chem. Phys. Lett.* **110**, 546 (1984).

⁷A. Hoshikawa, T. Kamiyama, A. Purwanto, K. Ohishi, W. Higemoto, T. Ishigaki, H. Imai, and K. Inoue, *J. Phys. Soc. Jpn.* **73**, 2597 (2004).

⁸C. Gonzalez, J. Campo, G. J. McIntyre, F. Palacio, Y. Numata, Y.

Yoshida, K. Kikuchi, and K. Inoue (unpublished).

⁹K. Ohishi, W. Higemoto, A. Koda, S. R. Saha, R. Kadono, K. Inoue, H. Imai, and H. Higashikawa, *J. Phys. Soc. Jpn.* **75**, 063705 (2006).

¹⁰Y. Yoshida, K. Inoue, and M. Kurmoo, *Chem. Lett.* **37**, 586 (2008).

¹¹M. Suzuki, *Prog. Theor. Phys.* **58**, 1151 (1977).

¹²Y. Miyako, S. Shikazawa, T. Saito, and Y. G. Yuochunas, *J. Phys. Soc. Jpn.* **46**, 1951 (1979).

¹³S. Fujiki and S. Katsura, *Prog. Theor. Phys.* **65**, 1130 (1981).

¹⁴J. L. García-Palacios and P. Svedlindh, *Phys. Rev. Lett.* **85**, 3724 (2000).

¹⁵J. Kishine, K. Inoue, and Y. Yoshida, *Prog. Theor. Phys.* **159**, 82 (2005).

¹⁶M. A. Girtu, C. M. Wynn, W. Fujita, K. Awaga, and A. J. Epstein, *Phys. Rev. B* **57**, R11058 (1998).